

Advanced Hot Reservoir Variable Conductance Heat Pipes for Planetary Landers

Kuan-Lin Lee¹, Calin Tarau², Andy Lutz³ and William G. Anderson⁴
Advanced Cooling Technologies, Inc, Lancaster, PA, 17601

and

Cho-Ning Huang⁵, Chirag Kharangate⁶ and Yasuhiro Kamotani⁷
Case Western Reserve University, Cleveland, OH, 44106

The next generation of Lunar rovers and landers requires variable thermal links to maintain payload temperatures nearly constant over wide sink temperature fluctuations. It has been demonstrated on earth that a hot reservoir variable conductance heat pipe (VCHP) can provide a much tighter passive thermal control capability compared to a conventional VCHP with cold-biased reservoir. However, previous ISS test results revealed that the fluid management of a hot reservoir VCHP needs to be improved to ensure its long-term reliability. Under an STTR Phase I program, Advanced Cooling Technologies, Inc. in collaboration with Case Western Reserve University performed fundamental research to understand the complex transport phenomena within a hot reservoir VCHP. A novel loop VCHP configuration was developed during the program. This loop design allows a net flow to be induced and circulate along the NCG tubing system, which will continuously remove the excessive working fluid from the reservoir (i.e. purging) in a much faster rate compared to diffusion alone. Two potential mechanisms to induce net transport flow were identified:

1. By momentum transfer from vapor to NCG through shearing in the condenser/front region. It was called “DC” mechanism.
2. By filtering the pulses (via a tesla/check valve) generated in the heat pipe section of VCHP loop. It was called “AC” mechanism.

Although these two mechanisms are independent, the AC mechanism can be further added/superimposed on the top of the DC mechanism to achieve a higher flow rate. This paper presents the work performed in Phase I to proof the existence of momentum transfer flow (“DC flow”) and its effectiveness on VCHP purging. The work includes theoretical analysis, numerical modeling, prototype development and experimental demonstration.

Nomenclature

AC	=	fluctuating component of the flow within a loop VCHP
DC	=	constant component of the flow within a loop VCHP
D	=	diffusion coefficient
L_{NCG}	=	length of NCG tube
R_{NCG}	=	internal radius of NCG tube
U	=	average induced flow velocity
μ	=	viscosity of NCG
ψ	=	vapor concentration in the reservoir

¹ R&D Engineer III, Advanced Cooling Technologies, Inc., 1046 New Holland Ave., Lancaster, PA 17601

² Principal Engineer, Advanced Cooling Technologies, Inc., 1046 New Holland Ave., Lancaster, PA 17601

³ R&D Engineer II, Advanced Cooling Technologies, Inc., 1046 New Holland Ave., Lancaster, PA 17601

⁴ Chief Engineer, Advanced Cooling Technologies, Inc., 1046 New Holland Ave., Lancaster, PA 17601

⁵ Graduate Student, Case Western Reserve University, 10900 Euclid Ave., Cleveland, OH 44106

⁶ Assistant Professor, Case Western Reserve University, 10900 Euclid Ave., Cleveland, OH 44106

⁷ Professor, Case Western Reserve University, 10900 Euclid Ave., Cleveland, OH 44106

Δp = pressure difference between inlet and outlet of NCG tube

I. Introduction

NASA's plans to further expand human and robotic presence in space automatically involve significant challenges. Spacecraft architectures will need to handle unprecedented thermal environments in deep space. In addition, there is a need to extend the duration of the missions in both cold and hot environments, including cis-lunar and planetary surface excursions. The heat rejection turn-down ratio of the increased thermal loads in the above-mentioned conditions is crucial for minimizing the usage of vehicle resources (e.g. power). Therefore, future exploration activities will need thermal management systems that can provide higher reliability and performance, and, at the same time, with reduced power and mass. To meet these requirements, passive thermal management concepts that offer large turn-down ratios are highly encouraged. As an example, the anchor node network (which is a lander that includes a seismometer, a laser reflector, and a probe for measuring heat flow from the Moon's interior) has a Warm Electronics Box (WEB) and a battery, both of which must be maintained in a fairly narrow temperature range. A variable thermal link between the WEB and radiator is required. During the day, the thermal link must transfer heat from the WEB electronics to the radiator as efficiently as possible, with minimum thermal resistance, to minimize the radiator size. On the other hand, the thermal link must be as ineffective as possible (provide as high thermal resistance as possible) during the Lunar night. This will keep the electronics and battery warm with minimal power, even with the very low temperature (100 K) heat sink. At this time, heat must be shared between the electronics and battery, to keep the battery warm. Moreover, since the cold lunar night is very long (14 days) minimizing or even eliminating the survival power is highly desired. This can be done with a passive variable thermal link between the WEB and the Radiator. This variable thermal link can be a hot reservoir variable conductance heat pipe (VCHP).

It was already demonstrated both analytically and experimentally^{1,2,3} that hot reservoir VCHPs would offer tight passive thermal control as opposed to the traditional cold biased reservoir VCHPs that, for the same tightness of thermal control need reservoir heating. Figure 1 (a) shows analytical thermal control predictions for two VCHP hot (Configuration 1) and cold (Configuration 2) reservoir designs with five different working fluids: Methanol, Toluene, Pentane, Ammonia and Propylene. As seen, the hot reservoir configuration shows a much narrower vapor temperature band compared to the cold reservoir configuration, as sink temperature sweeps vary between -90°C and 40°C.

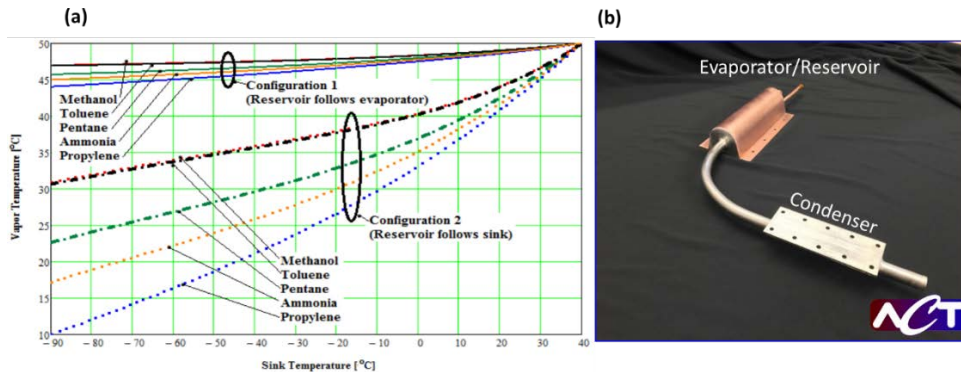


Figure 1. (a) Analytical thermal control predictions for two VCHP hot and cold reservoir configuration with five different working fluids: Methanol, Toluene, Pentane, Ammonia and Propylene³ (b) VCHP with an integrated hot reservoir for ISS test

The hot reservoir VCHP (Figure 1(b)) was tested on ISS in 2017 as part of the Advanced Passive Thermal experiment (APT_x) project⁴. While the ground testing was a success, the microgravity testing failed. The pipe showed higher than admissible temperatures that tripped the safety thermostats. The explanation of the failure is as follows: during startup, the absence of natural convection in the reservoir delayed the non-condensable gas (NCG) heating compared to vapor heating that is much more effective because of metallic (copper) path of the incoming heat. The consequence was that vapor pressure increased faster than NCG pressure (because of poor heating) and the resulted pressure wave pushed vapor into the reservoir (where colder NCG was present) where part of it condensed. As a result, the NCG was displaced out in the condenser increasing vapor temperature considerably. Next step was the attempt to remove vapor from the reservoir by applying heat to the reservoir, which is referred as “purging process”. It was found that the rate of purging was very low. The slow purging rate became a show stopper for the experiment.

Based on the ISS test results, it was concluded that fluid management within the reservoir and the NCG tube (typically non-wicked) of VCHPs is the key area to be improved. Advanced features/solutions that can (1) prevent

working fluid condensing inside a reservoir and (2) remove working fluid from the reservoir efficiently are needed to support foreseeable long-term warm reservoir VCHP space operations. Under this STTR program, Advanced Cooling Technologies, Inc (ACT) in collaboration with Case Western Reserve University (CWRU) perform a detailed and fundamental study to understand complex transport phenomena of multi-species within a hot reservoir VCHP. A novel “Loop hot reservoir VCHP” configuration resulted from this study, that can potentially enhance VCHP’s reliability in both ground and microgravity operations.

II. Loop Hot Reservoir VCHP Configuration

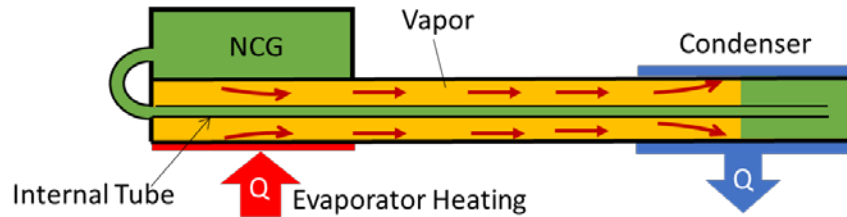


Figure 2. Regular VCHP with integrated warm reservoir (Green: NCG rich gas; Yellow: Vapor rich gas)

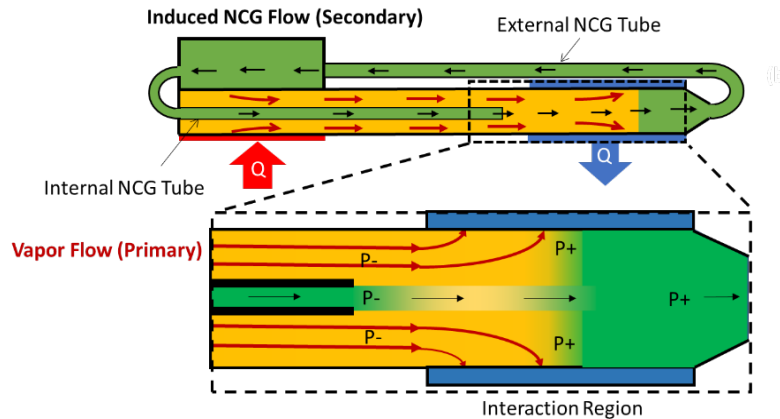


Figure 3. Loop Hot Reservoir VCHP (Green: NCG rich gas; Yellow: Vapor rich gas)

As depicted in Figure 2, a regular hot reservoir VCHP uses only one internal NCG tube connecting the reservoir with the condenser. A loop hot reservoir VCHP concept is illustrated in Figure 3. This novel configuration consists of a hot reservoir VCHP and two NCG tubes. One tube (internal) coming out from the NCG reservoir goes into the heat pipe section from the evaporator end. A second tube externally connects the end of the condenser with the reservoir. This loop configuration would allow a secondary (the vapor flow is considered as “primary”) fluid flow to be induced and move along the loop in the favorable direction (reservoir-internal tube-condenser) for purging (indicated with the black arrows). The mechanism to induce the secondary flow (i.e. transport flow) is as follows,

1. A strong vapor flow (i.e. primary flow) is generated in the heat pipe section due to evaporation and condensation of the working fluid.
2. The primary flow will carry momentum in axial direction. As the vapor passes by the end of internal NCG tube, some of the momentum will be transferred to the NCG stream through the shear between two species as well as a low static pressure point is created at the end (entrance) of the NCG tube.
3. Both the momentum transfer from vapor flow to NCG at the interaction region (shown in Figure 3) as well as the low pressure point would induce a flow of NCG in a preferential direction.

Compared to the primary flow (vapor) velocity, the secondary flow (mostly NCG) is relatively weak but it would still be beneficial for VCHP purging in the following aspects,

- a) During startup, this flow will condition the VCHP by transporting NCG-vapor mixture from the reservoir to the condenser via the internal NCG tube. This reduces the vapor concentration (NCG humidity) in the reservoir by bringing dryer NCG from the condenser via the external tube.

- b) This secondary flow exists all the time as long as vapor flow exists within the heat pipe section. Therefore, the vapor concentration within the reservoir can be maintained at low (design) values all the time.
- c) Based on above described mechanism, heating of the reservoir (to encourage purging) may be eliminated.
- d) This convective-based purging will be significantly more effective than the diffusion-based purging. Diffusion is basically governed by concentration gradient between reservoir and condenser, so the rate of purging will decay as the concentration gradient decreases. But the convection-based purging rate is all thermally driven for as long as power/heat is transferred by the VCHP.

III. Concept Feasibility Study – Numerical and Theoretical Analysis

A. Diffusion-based Purging Model

To study the purging process of a hot reservoir VCHP, a CFD-based model was developed and by CWRU. The computational domain is shown in Figure 4. For simplicity, an axisymmetric model was considered where a thin NCG pipe is connected to a cylindrical reservoir at the center. This is a simplified version of the heat pipe internal tube, condenser and reservoir sections. The NCG pipe is cooled at the other end, which induces the condensation of the vapor. It is assumed that a uniform mixture of vapor and NCG exists before the cooling. After the start of cooling, the concentration of the vapor decreases gradually starting from the cooling section. Eventually, by diffusion process, the vapor concentration of the whole system is reduced to the value dictated by the cooling section temperature.

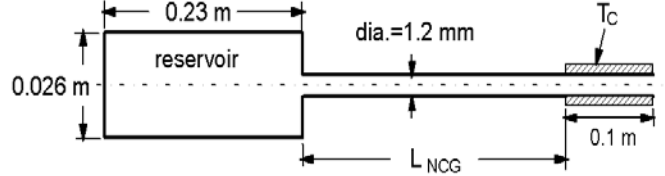


Figure 4. Computational domain of purging model

The vapor concentration (ψ) is determined by solving the diffusion equation.

$$\frac{\partial \psi}{\partial t} = D \nabla^2 \psi \quad (1)$$

The diffusion coefficient, D , changes with the temperature and pressure within the system.

$$D = D_0 \left(\frac{T}{T_0} \right)^{1.75} \frac{P_0}{P} \quad (2)$$

where $D = D_0$ at $T_0 = 273 \text{ K}$ (0°C) and $P_0 = 1 \text{ atm}$ (101 kPa). Except for the condenser, all other walls are assumed to be insulated. A mixture of water vapor and helium (NCG) is considered in the present analysis. Before the cooling starts, the mixture everywhere is assumed to be 50% water vapor and 50% helium at a temperature of 30°C . After time = 0, the cooling wall temperature is set at 10°C . For this mixture, D_0 is estimated to be equal to $2 \times 10^{-5} \text{ m}^2/\text{s}$. The mixture temperature changes from 30°C to 10°C in the process. The variation of vapor concentration within the reservoir is shown in Figure 5.

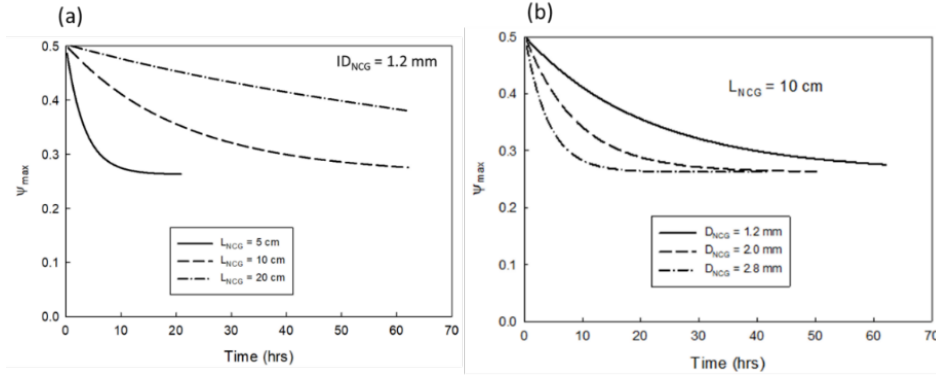


Figure 5. Variation of vapor concentration within reservoir with time for (a) various length of NCG tubes (ID 1.2 mm) and (b) various NCG tube diameters

Figure 5(a) shows how the values of ψ_{\max} change with time for several values of NCG pipe lengths. As the figure shows, diffusion (or purging) is a very slow process due to the fact that the mass transfer rate through the thin NCG pipe is limited. Although the total purging time depends on how we define the acceptable value of ψ_{\max} , the purging will take several days if the pipe length is longer than about 10 cm. The effect of the pipe diameter on the purging process is shown in Figure 5(b). As seen in the figure, a diameter of 2.8 mm reduces the purging time to around 15 hours. The analysis results demonstrated that the purging by diffusion may take tens of hours or even days, which matches ACT's past testing experience.

B. Numerical Study of Hot Reservoir VCHP Loop

Another numerical model is developed by CWRU to study the interaction between vapor and NCG within a hot reservoir VCHP and verify the momentum inducing flow mechanism described in the previous section. The computational domain is shown schematically in Figure 6. In this study the working fluid is acetone and the NCG is helium. The working temperatures are: 50, 60, 70, 80°C. It is assumed that the heat pipe operates in a gravity-assisted mode, so there is no wick structure. The pipe wall is made of aluminum. The relevant dimensions of the loop VCHP are summarized in Table 1. The amount of NCG is arbitrarily determined such that the vapor-NCG interface is located halfway in the condenser section at 50°C. The interface moves more into the condenser section with increase in operating temperature. The cooling is assumed to be done by forced convection cooling with specified heat transfer coefficient. The heat transfer coefficient is specified such that the heat input is nearly equal to 30W at 50°C with the ambient temperature equal to 20°C. Since the phenomena in the evaporator are not the focus in the present study, it is assumed that the evaporator simply generates enough vapor to balance the amount of condensation in steady state, so that the vapor flow is analyzed only in the adiabatic and condenser sections. The total pipe length (heat pipe and loop) is assumed to be 1 m. Since the NCG pipe is long and thin and the flow through the pipe is expected to be on the order of mm/s, the flow in the pipe can be assumed to be fully-developed. Therefore, instead of analyzing the pipe flow in detail, the known pressure drop-velocity relation for fully-developed pipe flow is used. The relation can be written as

$$\bar{U} = \frac{R_{NCG}^2 \Delta p}{8\mu L_{NCG}} \quad (3)$$

The computed pressure difference (ΔP) within a heat pipe with internal NCG tube is about 0.1 Pa. Even though the pressure difference is small, it is enough to generate appreciable flow. For example, 0.1 Pa of pressure difference can induce around 3.4 mm/s of flow (calculated based on Equation (3)).

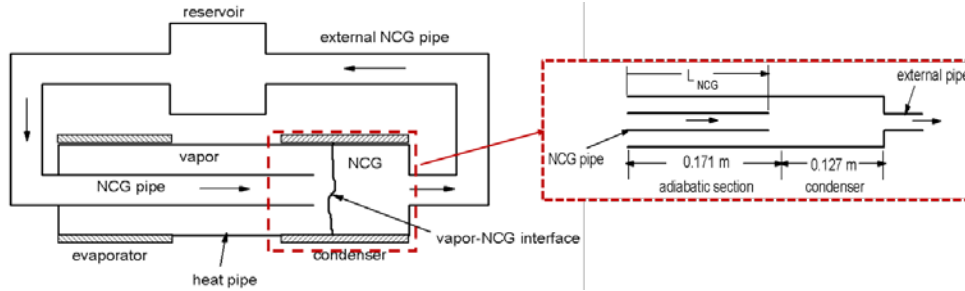


Figure 6. Schematic of VCHP loop

Table 1. Dimensions of hot reservoir VCHP Loop for numerical study

Geometric	Value (English)	Value (SI)
Evaporator length	4"	10.16 cm
Adiabatic length	6.75"	17.1 cm
Condenser length	5"	12.7 cm
Heat pipe OD	5/8"	1.59 cm
Heat pipe wall thickness	0.043"	0.11cm
NCG tube OD	1/4"	0.64 cm
NCG tube wall thickness	0.035"	0.09 cm

The dependence of the velocity on the NCG pipe outlet location is shown in Figure 7(a). The velocity increases as L_{NCG} becomes smaller. This happens because as the NCG pipe recedes (L_{NCG} becomes smaller), the friction effect on the vapor flow in the heat pipe decreases so that the stagnation pressure (or the pressure in the NCG region) increases. For the condition of Figure 7(a), the maximum velocity through the NCG pipe is about 4 mm/s. Figure 7 (b) shows how the velocity changes with Q while keeping T_{sat} constant. Q is changed from 8.9 to 41.5 W by changing the heat transfer coefficient for the cooling from 44 to 435 $Wm^{-2} \cdot K^{-1}$. The pipe flow velocity increases almost linearly with Q .

The effect of working temperature on the average NCG flow velocity is also numerically investigated. The relation between working temperature and induced NCG flow velocity when Q is fixed at 31W is presented in Figure 8(a). This figure shows that the velocity decreases with temperature. This occurs because as the vapor temperature increases, vapor density increases as well, which results in a decelerating vapor flow (for fixed Q) and therefore, the shearing effect on NCG decreases. To be noted is the fact that, in this case, the front goes away from the NCG tube which, according to modeling results, would increase the pressure difference. However, vapor velocity decrease dominates. Next, the combination effects of Q and the interface location with constant cooling rate is studied, which is shown in Figure 8 (b). As shown above, the effect of Q on the velocity is opposite to that of the interface location: increasing Q increases average flow velocity but moving vapor front further away the NCG tube end decreases the flow velocity.

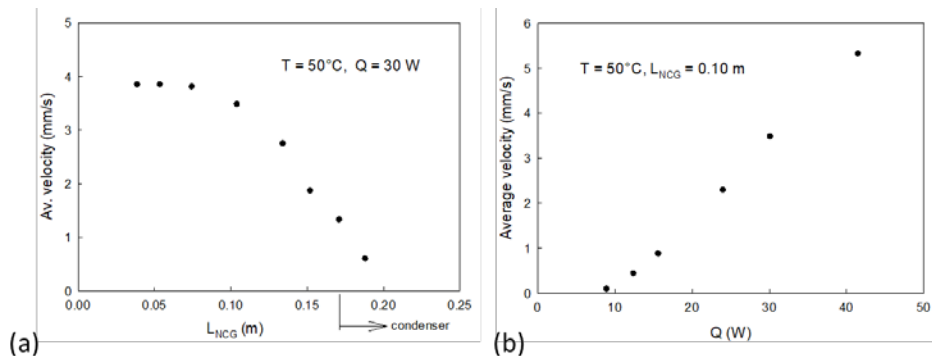


Figure 7. (a) Average velocity through NCG pipe vs. NCG pipe outlet location. (b) Average velocity through NCG pipe vs. heat input

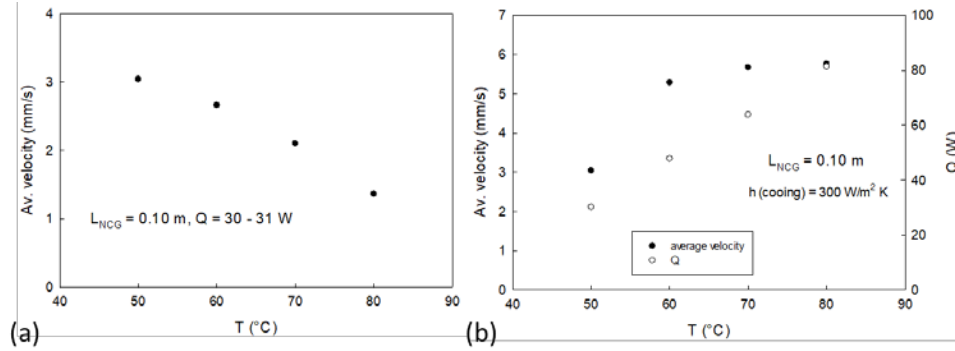


Figure 8. (a) Induced flow velocity vs. temperature with constant Q (b) Induced flow velocity and Q vs. temperature with constant heat transfer coefficient for cooling

Axial velocity profile along the cross-section A-A (aligned with the NCG pipe outlet) is presented in Figure 9. Since the NCG flow coming out from the internal tube is very small compared to the primary vapor velocity ($\sim 0.25 \text{ cm/s}$), it is very difficult to observe in the figure that there is a non-zero velocity near the center core ($r = 0$). In summary, utilizing this loop based VCHP concept, it is possible to obtain a sufficiently large velocity through the external pipe so that the purging can be accomplished within several minutes, which represents a significant improvement compared to the diffusion-based purging process discussed above. It is also found through simulation that multiple design parameters will affect the induced flow velocity, including

- Internal NCG tube end location and vapor front location.
- Heat input.
- Vapor temperature.
- Annular space between heat pipe and NCG tube.
- Gravity level and orientation of the pipe.

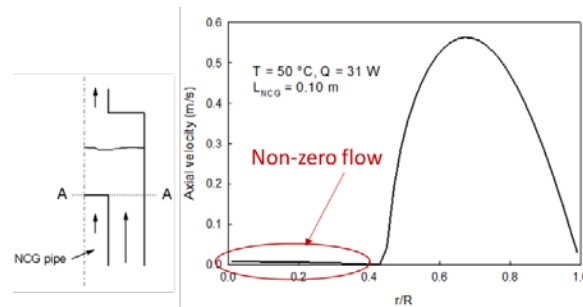


Figure 9. Velocity distribution across A-A section (induced flow velocity in the center is around 3 mm/s)

IV. Concept Feasibility Study – Experimental Validation

A. Experimental apparatus

In parallel to the mathematical study, an experimental demonstration was conducted by ACT to prove the existence of the momentum transport flow within a VCHP Loop. The schematic experimental system is shown in Figure 10 and the actual test setup is shown in Figure 11. The test apparatus consists of a VCHP with a non-integrated reservoir and an external NCG tube connecting between the condenser and the reservoir. The structural material is stainless steel. Working fluid and NCG are acetone and helium. The heat pipe section is in a slight gravity-aid orientation ($< 5^\circ$) and there is no wick structure inserted within the adiabatic and condenser sections for liquid return. According to the findings from numerical analysis (Figure 7(a)), the internal NCG tube length was adjusted so it ends in the adiabatic section before the condenser to obtain a higher induced flow velocity. Temperatures at various locations along the heat pipe and the loop are measured by 26 TCs. Key dimensions of the test setup are summarized in Table 2.

To measure the secondary flow induced by the primary vapor flow, a gas flow transducer (Omega FMA 1702A) is mounted in the line of the external NCG loop. This flow meter has no moving parts and uses thermal-based

technique to measure gas flow rate (hot wire anemometry). The measurement range of this flow meter is 0 to 10 cc/min. A very important fact is that this flow meter measures flow in only one direction. It allows however reverse flow but it reports “zero” flow rate in the DAQ system.

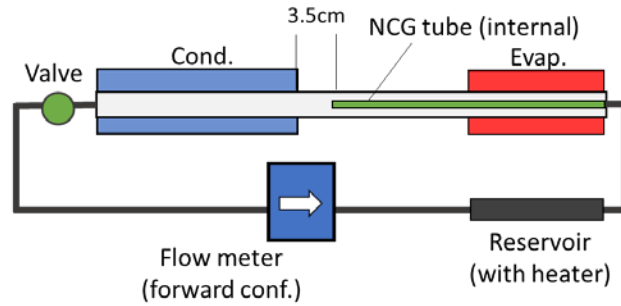


Figure 10. Schematic of experimental apparatus for Loop VCHP concept feasibility demonstration



Figure 11. Experimental apparatus of the VCHP loop concept demonstration

Table 2. Dimensions of the component of the VCHP Loop experimental apparatus

Internal NCG tube ID	0.18" (0.46cm)
Internal NCG tube OD	1/4" (0.64cm)
External NCG tube ID	Same as Internal tube
External NCG tube OD	Same as Internal tube
Heat pipe ID	0.46" (1.17cm)
Heat pipe OD	1/2" (1.27 cm)
Reservoir pipe ID	0.68" (1.73 cm)
Reservoir pipe OD	3/4" (1.91 cm)

B. Thermal Control Capability Demonstration

A thermal control testing is performed to assess/verify that adding an external NCG loop to hot reservoir VCHPs will not compromise thermal control capability of the VCHP. Figure 12(a) shows the operation of the VCHP loop at 80 W. At $t = 2200$ seconds, sink temperature is suddenly decreased from $75\text{ }^{\circ}\text{C}$ to $-10\text{ }^{\circ}\text{C}$. As the figure shows, the variation of evaporator temperature is less than $10\text{ }^{\circ}\text{C}$. Instantaneous temperature profiles of the heat pipe at steady state before and after decrease of sink temperature are shown in Figure 12(b). It can be observed that the vapor NCG front is located beyond the end of the condenser during the hot sink temperature mode before the step change. Then, the vapor NCG-front moves to reduce the active condenser length after the sink temperature drops. The new front is located at end of adiabatic section. Based on these test results, it is reasonable to state that adding an external NCG loop to a hot reservoir VCHP has minimal impact on its thermal control capability.

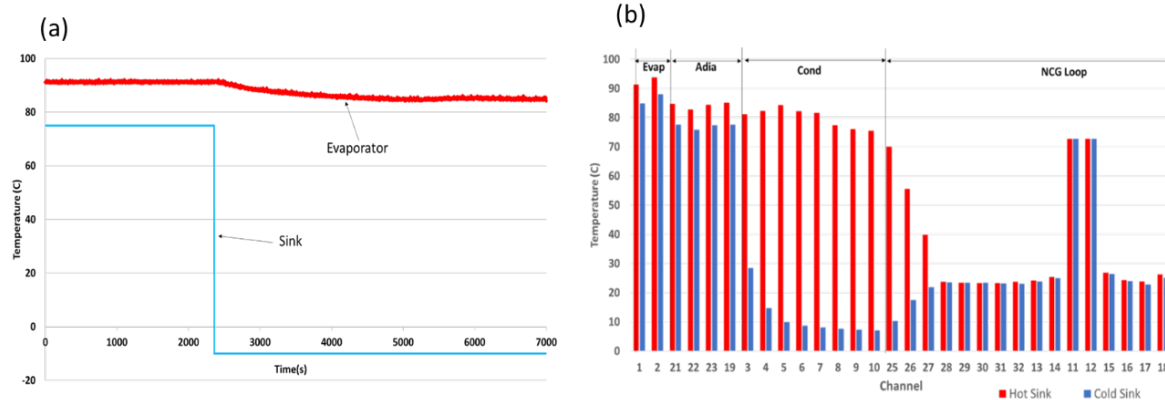


Figure 12. (a) VCHP test loop operation at 80 W with step change in sink temperature (b) Instantaneous heat pipe temperatures of VCHP test loop at 75 °C hot sink temperature and -10 °C cold sink temperature

C. Flow Measurements

Figure 13 shows the temperature evolution of the Loop VCHP and the corresponding flow rate measured by the flow meter. For this test, an amount of 6 ml of acetone was charged.

- (1) As the vapor/NCG is established within the condenser (shown as a purple line merging with the light blue line), an oscillating flow is observed.
- (2) The amplitude of oscillations is at around 1.5 sccm before the valve connecting heat pipe and loop is closed.
- (3) Immediately after closing the valve ($t = 8200$ sec), the amplitude dramatically increases.
- (4) As mentioned above, the flow meter cannot detect the flow in the opposite direction. All the “zero” values observed in this plot indicate that a reverse flow is passing the flow meter.

Flow test results reveal that the flow within the current Loop VCHP is a pulsating flow. One of probable causes of these pulses is the puddle formation in the evaporator. Since the heat pipe is slightly tilted, excessive working fluid liquid will accumulate at the bottom of evaporator and form a puddle. The expansion and collapse of bubbles might generate pressure waves. Another hypothesis of the origin of these pressure waves is the liquid slug forming in the condenser. Both phenomenon (puddle and slug formation within a heat pipe) are gravity-dependent and related to wick design. In microgravity, puddles and slugs might not form within a wicked heat pipe (either sintered powder or screen). However, liquid bodies and slugs could form within a grooved heat pipe in microgravity. Further investigation/assessments are needed for future space and planetary applications. This pressure wave generated from the heat pipe section propagates through the NCG tubes. The response of flow in the NCG tube will change depending on the status of the valve

- **If the valve is open**, the pressure wave will propagate through both sides of NCG tube (external and internal) and partially cancel each other. The amplitude of the pulses is small.
- **If the valve is closed**, pressure wave will propagate through only one side of NCG tube (internal) and the flow meter will experience a higher amplitude of oscillation.

Based on this finding, two potential mechanisms associated with Loop VCHP configuration to induce/enhance a net flow for purging are identified:

- (1) Flow induced by the momentum generated in the NCG tube through pressure variation (original mechanism). This mechanism is called “DC” mechanism.
- (2) Flow induced by filtering (via a Tesla or a check valve) the pulse generated within the heat pipe section. This mechanism is called “AC” mechanism.

Note that the DC and AC mechanisms are independent in this context, meaning that they can be superimposed to induce a higher net mass flow rate within a loop VCHP.

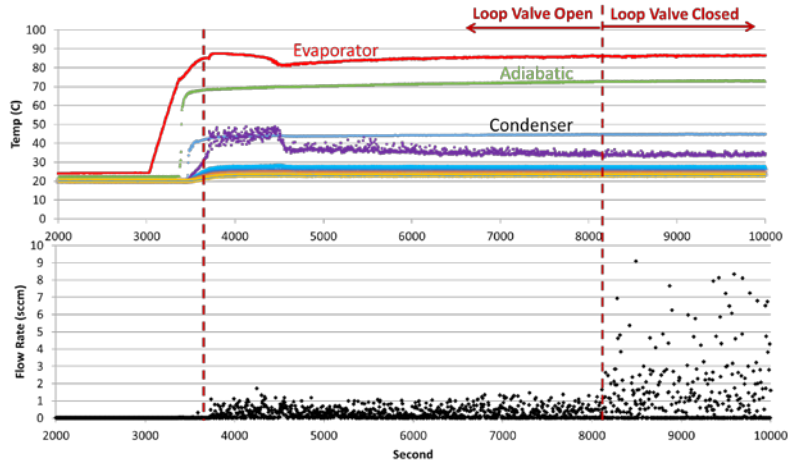


Figure 13. Temperature of VCHP Loop vs. secondary flow rate

D. Momentum Transfer Flow (DC Mechanism) Identification

The flow induced by DC mechanism is embedded within the total flow with pulses. In order to detect the flow, it is necessary to minimize the amplitude of the pulses. This is done by inserting a layer of screen mesh into the evaporator section and minimizing fluid inventory to avoid puddle formation in the evaporator. Test results are shown in Figure 14. The red line represents the heat input to the evaporator and the blue line represents the induced net flow rate. With a 2 ml of working fluid inventory, pulse amplitude is minimized to be within the resolution of the flow meter. A clear relationship between induced flow rate and the heat input can be identified. The flow rate of induced flow increases as the heat input increases. With 72W of heat input, the net flow velocity being induced is 0.8 cm/min (0.13 mm/s). All the evidence reach to the same conclusion: there is a net flow induced by the momentum transfer from the vapor to NCG within the Loop VCHP. The existence of DC flow is successfully proven.

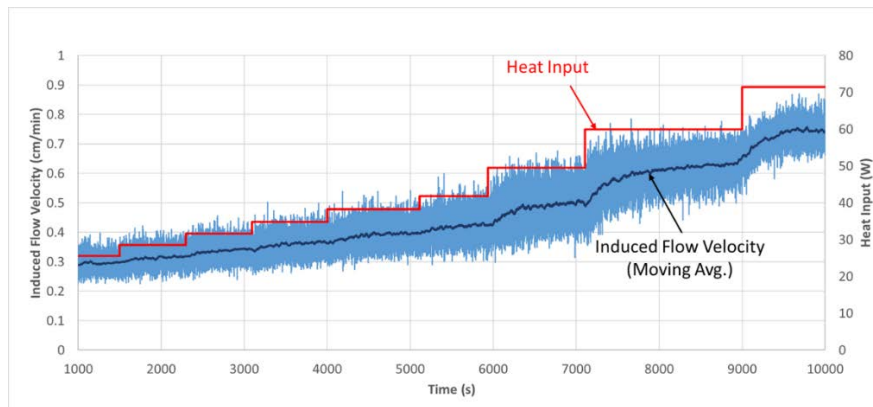


Figure 14. Momentum transport induced flow rate increases as the heat input increases

V. Prototype Development and Performance Demonstration

A hot Reservoir VCHP loop prototype is then developed for concept demonstration, which is shown in Figure 15(a). This VCHP prototype has an integrated reservoir similar to the VCHPs previously developed under another NASA Phase II program. This prototype consists of several parts, including reservoir, condenser, internal NCG tube, heat pipe adiabatic section and the external NCG tube. These parts are joined by Swagelok fittings, so they can be exchangeable. The working fluid is acetone and NCG is helium. No wick structure is inserted within the heat pipe adiabatic and condenser sections. liquid return is simply achieved by gravity. Similar to the loop VCHP experimental setup, a layer of screen is inserted into the evaporator to avoid puddle formation. There are two fill tubes in this prototype: one fill tube attached to the end of condenser is for working fluid and NCG charging; another fill tube welded on the top of reservoir is used for purging test only. The experimental system for VCHP prototype testing is shown in Figure 15(b). Heating to the evaporator is provided by a heater block from the bottom of the evaporator.

Cooling of the condenser is provided by a chiller block. The instrumentation includes 25 T-type TCs and the flow meter to measure the induced flow rate through the NCG loop. Two DAQ systems (one for temperature and one for flow meter) are simultaneously operating to collect both temperature and flow data.

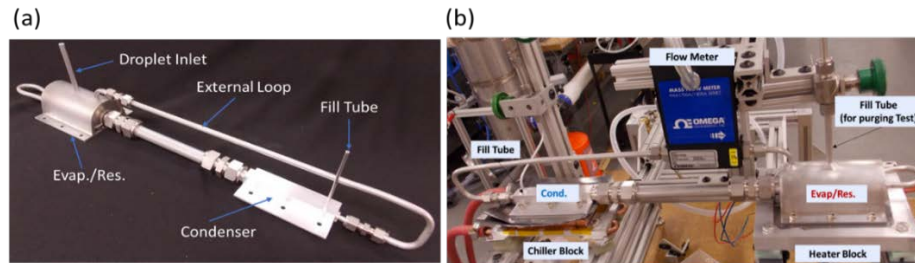


Figure 15. (a) Hot Reservoir VCHP Loop prototype (b) testing system

Purging performance of this prototype was tested and the results are shown in Figure 16. At $t=t_0$, heat input incrementally increases from 110W to 140W. At $t=t_1$, 0.3 ml of acetone, which is 12% of the working fluid inventory is directly injected into the reservoir. Immediately, payload temperatures increase and condenser temperatures decrease, meaning that the vapor front is pushed towards the adiabatic section decreasing the active length of the condenser. Monitoring payload temperature decaying rate between t_2 and t_3 it can be observed that the average dropping rate is around -4°C in 3000 seconds. The corresponding induced flow rate measured by the flow meter is around 0.16 ml/min. Compared to a regular hot reservoir VCHP without a loop, the purging speed of this prototype is 6.7 times faster. This test results conclude that new loop configuration and the induced flow concept does improve the purge rate and reliability of VCHP.

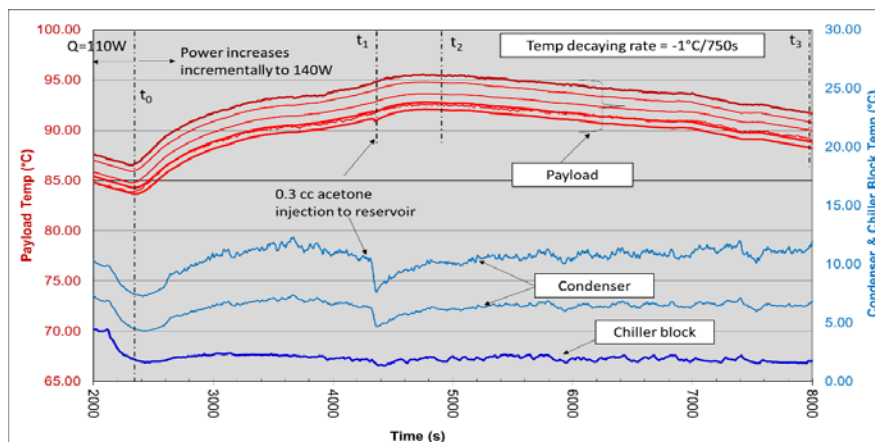


Figure 16. Purging performance of Hot Reservoir VCHP Loop

Still there is significant room for improvement. ACT and CWRU team believe that an even higher induced flow can be achieved by design optimization and implementation of other features (e.g. pulse filtering devices and nozzles etc.). Figure 17 below shows how effective the purging process would be if a transport flow can be induced within the Loop VCHP. This calculation assumes that an NCG reservoir volume of 100 c.c. contains 50% of vapor initially and the internal NCG tube (with 0.18"ID) has a length of 50 cm. Purging by diffusion will take roughly 24 hours to reduce vapor concentration within the reservoir from 50% to 35%. If a 0.5 mm/s of transport flow can be induced within the loop VCHP, it will only take 6 hours to achieve same level of concentration reduction (from 50% to 35%). If a 20 mm/s flow velocity within a VCHP loop can be achieved (through superimposing DC and AC mechanisms discussed above), purging time can be significantly reduced to less than 10 mins. To achieve a higher flow rate in the loop VCHP, ACT-CWRU team plans to (1) systematically study the momentum induced flow and identify influential design parameters (2) develop features that can amplify the momentum induced flow and (3) develop pulse filtering devices to obtain a net flow from pulses.

VI. Conclusion

Under this STTR Phase I, ACT and CWRU performed a fundamental investigation to understand the complex transport phenomena within a hot reservoir VCHP. In order to address the slow purging problem of a hot reservoir VCHP, a novel loop configuration is developed that uses an external NCG tube connecting the reservoir and the condenser to create a closed flow path for NCG to replenish reservoir. With the loop configuration, the momentum of vapor within the heat pipe section will generate a pressure difference that can induce a net NCG flow in a favorable direction for reservoir purging (i.e. removal of vapor from reservoir). Modeling results demonstrate the possibility of flow generation through momentum transport/transfer in a Loop hot reservoir VCHP. A Loop VCHP experiment is performed and following key findings are identified:

- Thermal control capability of hot reservoir VCHP is not affected by adding a loop.
- Flow within a hot reservoir VCHP loop is pulsating.
- The momentum transfer based induced flow is successfully identified using an accurate gas flow meter.

In addition, two independent mechanisms that can induce a net flow are identified:

1. By the momentum transfer from the vapor to NCG through shearing. This mechanism is called “DC” mechanism .
2. By filtering the pulses generated within Loop VCHP, using a fluid diode (e.g. Tesla valve). This mechanism is called “AC” mechanism.

These two mechanisms are independent, so they can be superimposed to induce a higher flow rate for purging. A proof-of-concept prototype that has an integrated evaporator and reservoir design similar to the hardware tested at ISS is developed. The thermal control capability and momentum induced flow of the prototype are experimentally demonstrated. The reliability of the prototype is also tested, which shows a 6.7 times of purging rate improvement compared to regular hot reservoir VCHP without loop and induced flow. If a 20 mm/s flow velocity within a VCHP loop can be achieved (through superimposing DC and AC mechanisms discussed above), purging time can be significantly reduced to less than 10 mins.

Acknowledgments

This project is sponsored by NASA Marshall Space Flight Center (MSFC) under an STTR Phase I program (Contract# 80NSSC18P2155). We would like to thank the program manager, Brian O'Connor and Dr. Jeff Farmer for their supports and valuable inputs during the program. Special appreciation goes to Philip Texter and Chris Jarmoski who have provided significant technical contributions to the program.

References

- ¹ Tarau C., Schwendeman C. L., Schifer N.A., Polak J. and Anderson W.G., “Optimized Back up Cooling System for the Advanced Stirling Radioisotope Generator”, in *International Energy Conversion Engineering Conference (IECEC)*, 2015
- ² Tarau C., Schwendeman C. L., Anderson W.G., Cornell P.A. and Schifer N.A., “Variable Conductance Heat Pipe Operated with Stirling Converter”, in *IECEC*, 2013
- ³ Tarau C. and Anderson W.G., “Variable Conductance Thermal Management System for Balloon Payload”, in *20th AIAA Lighter-Than-Air Systems Technology Conference*, 2013
- ⁴ Tarau C., Ababneh M.T., Anderson W.G., Alvarez-Hernandez A.R., Ortega S., Farmer J.T. and Hawkins R., “Advanced Passive Thermal eXperiment (APT_x) for Warm-Reservoir Hybrid-Wick Variable Conductance Heat Pipes on the International Space Station (ISS)” in *48th International Conference on Environmental Systems (ICES)*, 2018

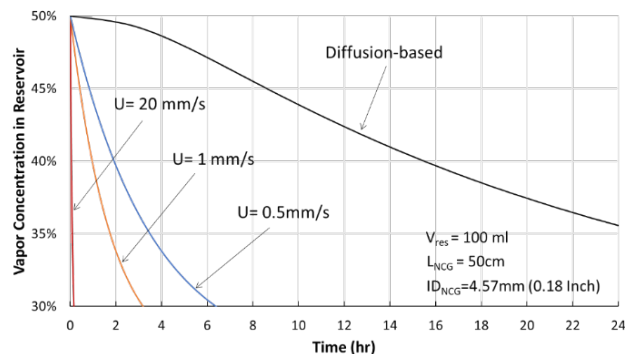


Figure 17. Convection-based purging rate vs. diffusion-based purging rate